

This is the author's final, peer-reviewed manuscript as accepted for publication (AAM). The version presented here may differ from the published version, or version of record, available through the publisher's website. This version does not track changes, errata, or withdrawals on the publisher's site.

Decay heat in ISIS spallation neutron target as function of cooling time

G M Allen, R A Burridge, D J S Findlay, D J Haynes,
D M Jenkins, G P Škoro and D Wilcox

Published version information

Citation: G Allen et al. "Decay heat in ISIS spallation neutron target as function of cooling time." Nuclear Instruments and Methods A, vol. 933 (2019): 8-11.

DOI: [10.1016/j.nima.2019.04.072](https://doi.org/10.1016/j.nima.2019.04.072)

©2019. This manuscript version is made available under the [CC-BY-NC-ND](https://creativecommons.org/licenses/by-nc-nd/4.0/) 4.0 Licence.

This version is made available in accordance with publisher policies. Please cite only the published version using the reference above. This is the citation assigned by the publisher at the time of issuing the AAM. Please check the publisher's website for any updates.

This item was retrieved from **ePubs**, the Open Access archive of the Science and Technology Facilities Council, UK. Please contact epubs@stfc.ac.uk or go to <http://epubs.stfc.ac.uk/> for further information and policies.

Decay heat in ISIS spallation neutron target as function of cooling time

G M Allen, R A Burridge, D J S Findlay, D J Haynes, D M Jenkins, G P Škoro
and D Wilcox

Rutherford Appleton Laboratory, Chilton, Didcot, OX11 0QX, UK

Abstract

Thermal power from radioactive decay ('decay heat') in an ISIS proton-driven spallation neutron target has been measured in a carefully controlled and consistent way as a function of cooling time between 1 minute and 2 weeks. Overall, results are in good agreement with calculations made with the Monte Carlo program MCNPX.

1. Introduction

For operational and safety-related reasons it is often necessary to know what the thermal power is from radioactive decays ('decay heat') within a target irradiated by a particle beam once the beam has been switched off, especially for a highly irradiated target on a high-power particle accelerator. Since they can be difficult to measure, especially on a working accelerator facility, decay heats are usually calculated by Monte Carlo computer codes such as MCNPX [1].

In a previous publication [2] we presented a comparison of two measured and calculated decay heats on the ISIS Spallation Neutron Source [3] immediately after beam switch-off. In the present publication, we present measurements and calculations of decay heats in the water-cooled twelve-plate tantalum-clad tungsten target in the ISIS First Target Station (TS-1) spanning a cooling-time range of 1 minute to 2 weeks. This target first saw beam in March 2015, and since then has been irradiated for ~4000–4500 hours a year by a ~180- μ A proton at 40 pulses per second (pps), although the usual 800-MeV energy of the ISIS proton synchrotron has sometimes been reduced to 700 MeV in order to reduce strain on the lattice dipoles. During irradiation the thermal power dissipated within the target is ~100 kW, and the target is instrumented with thermocouples that measure the temperature of each plate.

2. Measurements

The measurements described in the present publication were all made following the end of a 5-week continuous campaign for the ISIS users. At 08:30:15 on 20 December 2018 the proton beam being delivered to the target was switched off, at 08:31:20 the cooling water flow through the target was switched off, and the resultant rising temperatures from the plate thermocouples were recorded at 1-second intervals on a PLC-based system. At 09:00 the water flow was restored, and the water flow was subsequently switched off and on six more times as summarised in Table 1. No other changes were made to the target and its environment during the two weeks spanning the range of measurements. In spite of its operational inconvenience, such an arrangement was felt to offer the best chance of achieving self-consistency in a set

of decay heat measurements made over a time span of two weeks, as the irradiation history is the same for all seven different cooling times, and the heat transfer parameters associated with the target plates and their local environment should all be the same. A typical set of temperature curves is shown in Figure 1.

Data set #	Date	Water off	Water on	Cooling time
[20 Dec. 2018: beam off 08:30:15]				
1	20 Dec. 2018	08:31:20	08:59:55	1 min.
2	20 Dec. 2018	09:30:06	10:00:10	1 hour
3	20 Dec. 2018	11:30:21	12:00:17	3 hours
4	21 Dec. 2018	08:30:05	09:00:03	1 day
5	23 Dec. 2018	08:30:02	09:00:02	3 days
6	27 Dec. 2018	08:30:02	09:30:04	7 days
7	3 Jan. 2019	08:30:02	10:30:03	14 days

Table 1. Times during which water flow through the target was switched off and the plate thermocouple temperatures were recorded.

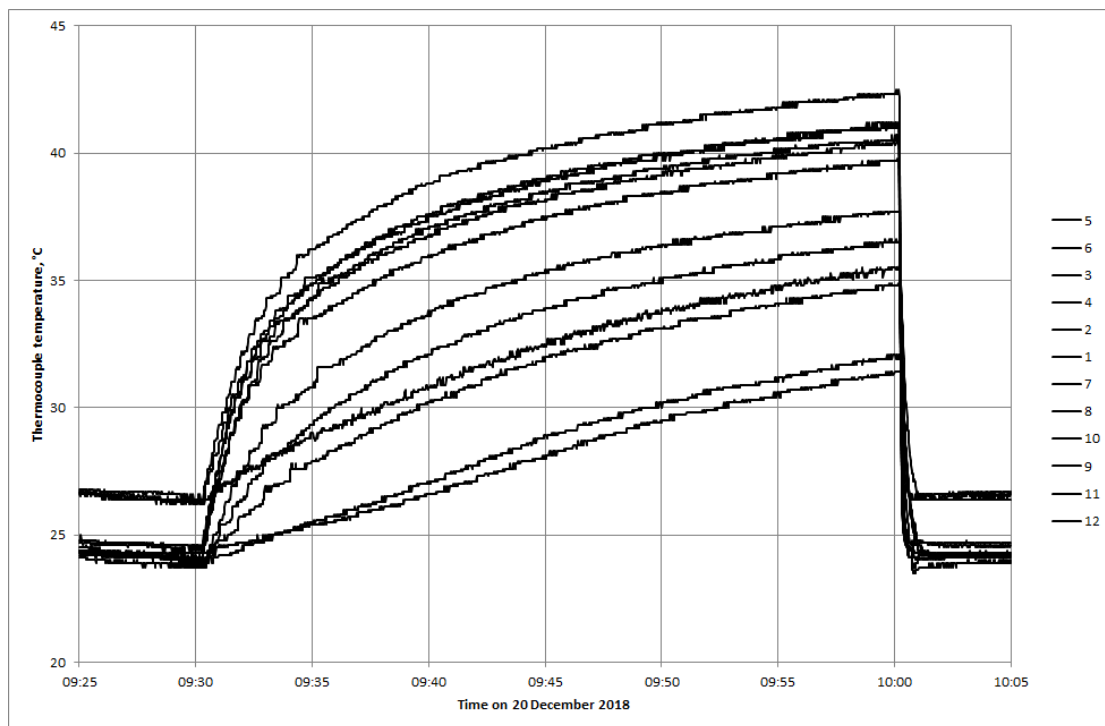


Figure 1. Target plate temperatures (data set #2 in Table 1) starting to rise at 09:30 when the cooling water flow was switched off 1 hour after the beam was switched off at 08:30 on 20 December 2018. The order of the curves at 09:50 is the same as the order of target plate numbers in the list at the right-hand side. Each curve consists of ~1800 data points spread over ~30 minutes.

3. Analysis

The coupled-two-mass model developed previously [2] was fitted to the seven sets of measured temperature data. In this model, each target plate can exchange heat with its two neighbours¹, and exchange heat with the target pressure vessel; further, the pressure vessel can exchange heat with a local heat sink. The model is characterised by the following set of $n + 1$ differential equations for $\dot{T}_i = dT_i/dt(t)$ where T_i is the temperature of plate i , t is time, and n is the number of plates:

$$\begin{aligned}
 \dot{Q}_1 &= m_1 c_1 \dot{T}_1 + \beta_{1,2}(T_1 - T_2) + \alpha_1(T_1 - T_v) \\
 \beta_{1,2}(T_1 - T_2) + \dot{Q}_2 &= m_2 c_2 \dot{T}_2 + \beta_{2,3}(T_2 - T_3) + \alpha_2(T_2 - T_v) \\
 &\vdots \\
 \beta_{i-1,i}(T_{i-1} - T_i) + \dot{Q}_i &= m_i c_i \dot{T}_i + \beta_{i,i+1}(T_i - T_{i+1}) + \alpha_i(T_i - T_v) \\
 &\vdots \\
 \beta_{n-2,n-1}(T_{n-2} - T_{n-1}) + \dot{Q}_{n-1} \\
 &= m_{n-1} c_{n-1} \dot{T}_{n-1} + \beta_{n-1,n}(T_{n-1} - T_n) + \alpha_{n-1}(T_{n-1} - T_v) \\
 \beta_{n-1,n}(T_{n-1} - T_n) + \dot{Q}_n &= m_n c_n \dot{T}_n + \alpha_n(T_n - T_v) \\
 \\
 \sum_{i=1}^n \alpha_i(T_i - T_v) &= m_v c_v \dot{T}_v + \gamma(T_v - T_s)
 \end{aligned}$$

where the α 's represent thermal conductances between the target plates and the target pressure vessel, the β 's represent thermal conductances between pairs of plates, γ represents the thermal conductance between the pressure vessel and the surroundings or thermal sink, c 's and m 's are specific heats and masses, and subscripts i , v and s refer to plate number, pressure vessel and thermal sink respectively. Solutions of this set of $n + 1$ coupled first-order linear differential equations obtained using the Harwell Subroutine Library (HSL) [4] routine DC04 were simultaneously fitted to the temperature data as functions of time for all twelve² target plates with the aim of extracting parameters of the fit, especially the decay heats \dot{Q}_i , and the function minimised during the fitting process was $\chi_{\text{pdf}}^2 = (\sum_{j,i} (T_{j,i}^{\text{data}} - T_{j,i}^{\text{fit}})^2 / \delta T_{j,i}^2) / (n_{i \times j} - n_{\text{param}})$ where the sum is taken over temperature data points j for plate numbers i , $\delta T_{j,i}$ was taken as 0.1°C for all j and i since the temperature data were recorded with a resolution of 0.1°C , $n_{i \times j}$ is the total number of temperature data points for all plates, and n_{param} is the number of parameters fitted. A total³ of 41 parameters were fitted: β (all β 's were assumed to be the same), γ , m_v , $T_v^{(0)}$, T_s , $T_1^{(0)}$, $T_2^{(0)}$, \dots , $T_{12}^{(0)}$, α_1 , α_2 , \dots , α_{12} , \dot{Q}_1 , \dot{Q}_2 , \dots , \dot{Q}_{12} , where the $T^{(0)}$'s are temperatures⁴ at time $t = 0$. Masses m 's and specific heats c 's are given in Table 2.

¹ Except, obviously, for the first and last plates in the target core.

² Only plates 1–10 were fitted in the previous publication [2].

³ Of course, only a few of the total number of parameters are fitted to the temperature data for each individual plate. For each plate, in round terms, ~ 4 parameters are fitted per ~ 1800 data points.

⁴ The $T^{(0)}$'s were included as parameters in order to mop up the consequences firstly of assuming that at any given time t there were no variations in temperature throughout a target plate and secondly of neglecting finite stopping times of water flow between pairs of plates. Fitted values of the $T^{(0)}$'s were typically less than 1°C different from the measured values.

Plate no.	Thickness, Ta + W + Ta, mm	m , g	c , J g ⁻¹ °C ⁻¹
1	2.0 + 11.0 + 2.0	3350	0.1366
2	2.0 + 11.0 + 2.0	3350	0.1366
3	2.0 + 12.0 + 2.0	3570	0.1365
4	2.0 + 13.5 + 2.0	3900	0.1364
5	2.0 + 15.0 + 2.0	4240	0.1363
6	2.0 + 18.0 + 2.0	4900	0.1362
7	2.0 + 21.0 + 2.0	5570	0.1360
8	2.0 + 26.0 + 2.0	6680	0.1359
9	2.0 + 34.0 + 2.0	8450	0.1358
10	2.0 + 40.0 + 2.0	9780	0.1357
11	2.0 + 46.0 + 2.0	11110	0.1357
12	2.0 + 46.0 + 2.0	11110	0.1357
Vessel			0.50

Table 2. Thicknesses of the twelve tantalum-clad tungsten target plates that comprise the target core, masses, and specific heats. The plates are 108 mm wide and 111 mm (on average) high, and each plate is separated from its neighbours by 2.0 mm of heavy water. Specific heats c vary very slightly with plate numbers because c_W is slightly smaller than c_{Ta} and the tungsten plates become thicker towards the back of the target whereas the thickness of tantalum cladding remains the same. The pressure vessel is stainless steel, hence the different specific heat. A diagrammatic representation of the target is given in [2].

Since many parameters are involved, and it is anything but easy to visualise the multi-dimensional surface wherein minima are sought, it is important that the minimisation routine used to match the model to the data can be relied upon. Two HSL minimisation routines were therefore used, VA04 and VA10, which work in different ways [5]. Although starting values for the minimisation for the α 's, β and γ of ~ 2 – 5 , ~ 10 and ~ 10 W °C⁻¹ respectively obtained from simple conduction and convection considerations were tried initially, better fits were obtained with starting values for the α 's, β and γ of ~ 20 , ~ 20 and ~ 50 W °C⁻¹ respectively. Starting values for the minimisation of the \dot{Q}_i 's were taken from Monte Carlo calculations. VA10 was found to lead to substantially lower values of χ_{pdf}^2 and substantially smaller spreads in parameter values, and to be noticeably faster, although VA04 and VA10 gave similar results for the decay heat $\dot{Q}_{tot} = \sum_i \dot{Q}_i$ for the target as a whole. Consequently, the results for $\dot{Q}_{tot} = \sum_i \dot{Q}_i$ given in Table 3 and in Figure 2 are the VA10 results. Uncertainties in \dot{Q}_{tot} were obtained by re-fitting one hundred times with all starting parameters randomly varied over a total range of half an order of magnitude and then taking the standard deviation of the resultant set of one hundred values of \dot{Q}_{tot} .

Another set of values of $\dot{Q}_{tot} = \sum_i \dot{Q}_i$ was derived from an ‘adiabatic’ approximation, whereby values of \dot{Q}_i were obtained simply by multiplying the initial rate of rise of temperature of each plate by the thermal capacity of the plate, *i.e.* by multiplying $\dot{T}_i(0)$ obtained directly from the temperature data curves by the product $m_i c_i$. However, in this approximation the vessel and its surroundings are neglected, and so it is hardly surprising that these ‘adiabatic’ results also shown in Figure 2 are significantly lower than the results obtained when the materials surrounding the target plates are included.

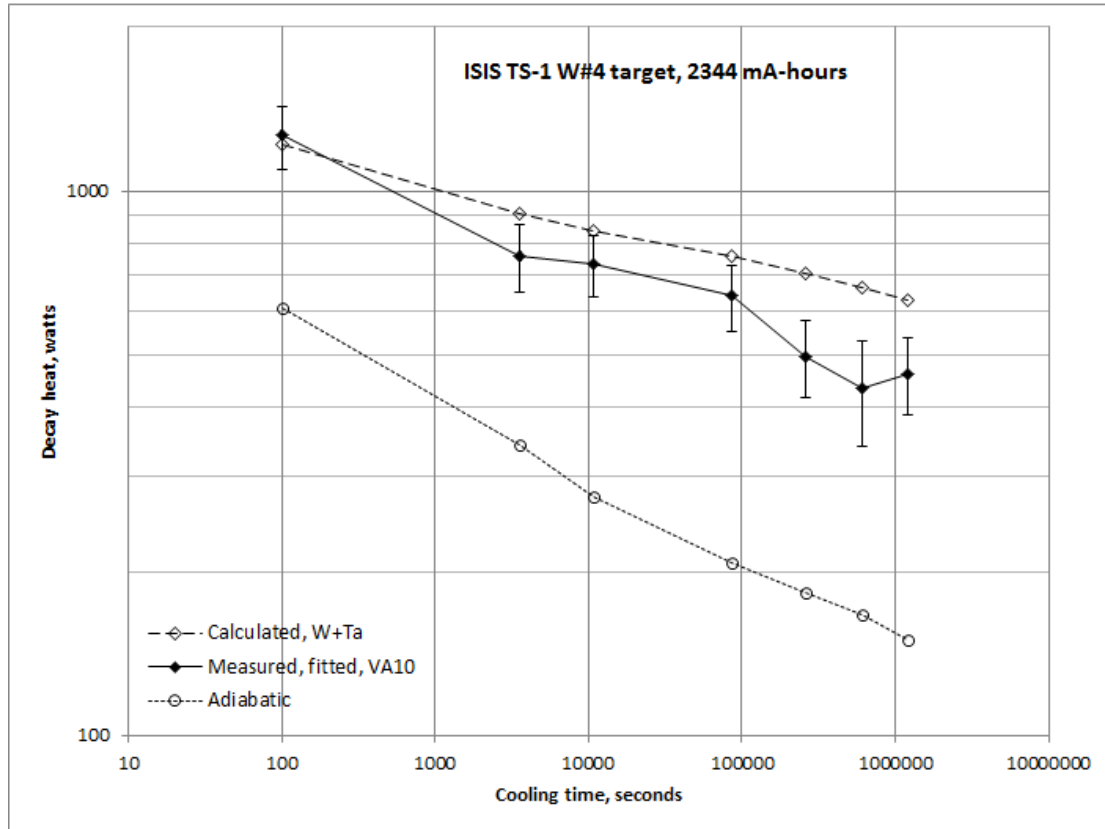


Figure 2. Measured and calculated values of decay heat for the ISIS TS-1 target as a function of cooling time after beam switch-off. The measured values were obtained from fits to temperature data as described in the text and the calculations were carried out using MCNPX. (The adiabatic curve was obtained as described in the text.)

Cooling time	Measured, VA10		Calculated \dot{Q}_{tot} , watts
	\dot{Q}_{tot} , watts	χ^2_{pdf}	
1 min.	1265 ± 165	1.27	1220
1 hour	760 ± 110	0.93	910
3 hours	735 ± 95	0.78	845
1 day	640 ± 90	0.72	760
3 days	495 ± 80	1.09	705
7 days	435 ± 95	1.06	665
14 days	460 ± 75	0.95	630

Table 3. Values for decay heat (watts) in the tungsten and tantalum target core and the corresponding goodness-of-fit parameter obtained by fitting the coupled-two-mass model to the measured temperature data, and calculated results from MCNPX. The numbers have been rounded to nearest multiple of five. The χ^2_{pdf} values of ~ 1 show that very good fits to the measured temperature curves are being obtained. Typical fitted values for the α 's and β were $\sim 4 \text{ W } ^\circ\text{C}^{-1}$ and $\sim 7 \text{ W } ^\circ\text{C}^{-1}$ respectively, not inconsistent with estimates from simple conduction and convection considerations; typical fitted values for γ were $\sim 90 \text{ W } ^\circ\text{C}^{-1}$, noticeably greater than estimates from simple considerations that, however, neglected the effect of the vessel surroundings; and typical fitted values of m_v were $\sim 120 \text{ kg}$, not inconsistent with the total mass of $\sim 200 \text{ kg}$ for the vessel and its associated flange.

4. Discussion

As in the previous publication, calculations of decay heat were carried out using the MCNPX Monte Carlo code [1] in association with the CINDER'90 transmutation code [6] and using a very detailed model of the ISIS TS-1 target-reflector-and-moderators (TRAM) assembly. The calculations took account of the detailed irradiation history of the target since the target was first irradiated in March 2015.

Overall, as can be seen in Figure 2, the agreement between the measured and calculated decay heats is good, although the measurements may be suggesting that MCNPX slightly overestimates the decay heat for longer cooling times.

The measurements also suggest a plausible dependence of decay heat within the target core as a function of depth into the target. Figure 3 shows individual measured values of \dot{Q}_i (from VA10) for four cooling times, and Table 4 gives the trend of the measured decay heat with increasing distance into the target for all seven cooling times. Also shown in Figure 3 are the values of \dot{Q}_i calculated by MCNPX. On the whole there is reasonably good agreement between measurement and calculation, although the uncertainties on data points are not negligible⁵. For short cooling times, the decay heat is concentrated at the front of the target, but as the cooling time becomes longer the decay heat becomes distributed more uniformly — consistent with the premise that short-lived spallation products are associated with the higher proton energies at the front of the target, whereas at longer cooling times the decay heat is dominated by ^{182}Ta which arises primarily from neutron capture and is more uniformly distributed throughout and around the target core.

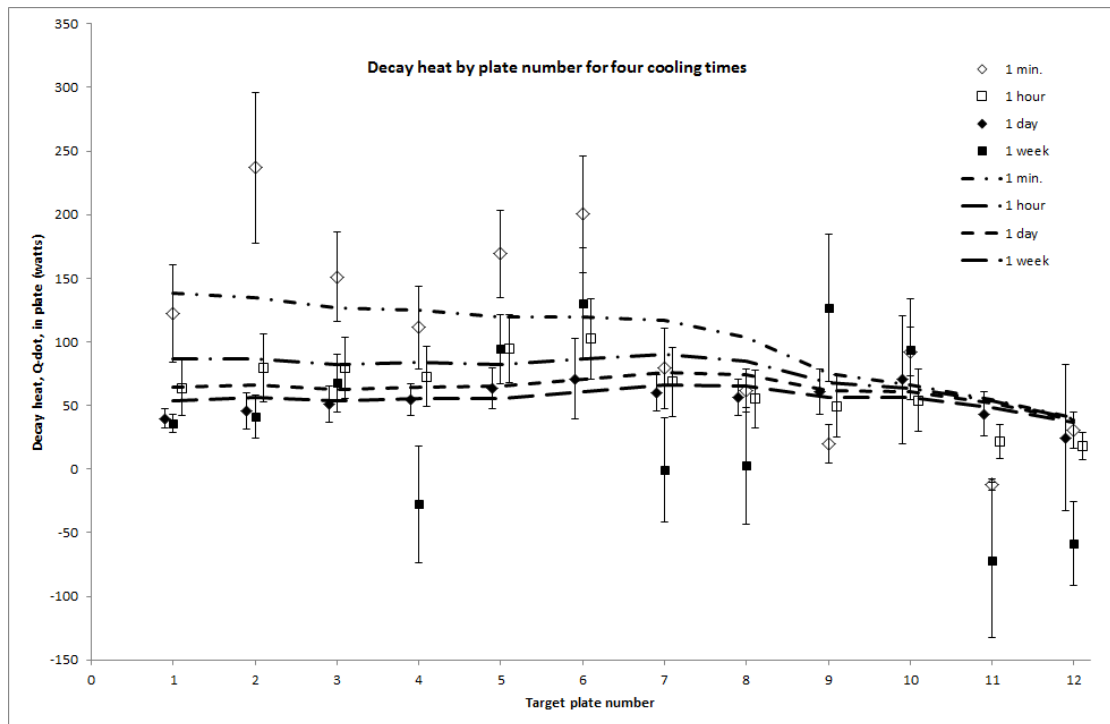


Figure 3. Decay heat for each target plate for four different cooling times. Data points, measurements; lines, MCNPX calculations.

⁵ There are substantial anti-correlations amongst the values of \dot{Q}_i extracted from the fitting procedure, so that the relative uncertainty in $\dot{Q}_{\text{tot}} = \sum_i \dot{Q}_i$ is much smaller than the relative uncertainties in the individual \dot{Q}_i .

Cooling time	Slope of \dot{Q}_l (in watts) as function of target plate number
1 min.	-16.0 ± 3.7
1 hour	-5.2 ± 1.0
3 hours	-2.5 ± 0.5
1 day	-0.2 ± 3.0
3 days	-6.7 ± 4.4
7 days	-5.3 ± 3.8
14 days	-6.8 ± 2.8

Table 4. Slope of linear fit to measured decay heat as function of plate number, *i.e.* a rough approximation to the slope of \dot{Q}_l as function of depth into the target, as a function of cooling time. The more negative is the slope, the more concentrated is the decay heat towards the front of the target.

Whilst it has been set up to represent the primary heat-flow paths within the target core and its surroundings, the coupled-two-mass model is of course ultimately a phenomenological model in which all the complicated details of time-dependent heat flow throughout a highly heterogeneous assembly are rolled up into set of plausible parameters whose values are effectively decided by the fitting process itself and amongst which significant correlations and anti-correlations can occur. Nevertheless, the coupled-two-mass model undoubtedly fits the measured temperature data very well, and its use allows values of decay heat to be extracted whilst taking the surroundings of the target core into account.

And, in a wider context, it is clear that the present seven sets of carefully and consistently acquired temperature measurements represent a valuable body of data on decay heat against which future models can be tested.

5. Conclusions

Thermal power from radionuclide decay ('decay heat') in a proton-driven tungsten target on a spallation neutron source has been measured in a carefully controlled and consistent way as a function of cooling time. The results suggest that the Monte Carlo code MCNPX is a reliable predictor of decay heat.

References

- [1] MCNPX 2.7.0 — Monte Carlo N-Particle Transport Code System for Multi-particle and High Energy Applications, <https://mcnpx.lanl.gov/>.
- [2] D J S Findlay *et al.*, Nucl. Instr. Meth. A908 (2018) 91.
- [3] <https://www.isis.stfc.ac.uk/>.
- [4] <http://www.hsl.rl.ac.uk/>.
- [5] 'FORTRAN Subroutines for Minimisation by Quasi-Newton Methods', R Fletcher, report AERE R 7125, UK Atomic Energy Authority, 1972.
- [6] W L Wilson *et al.*, Proc. SARE4 Workshop, Knoxville, USA, 1998.